TOPICAL REVIEW — Magnetism, Magnetic Materials, and Interdisciplinary Research

# Novel magnetic vortex nanorings/nanodiscs: Synthesis and theranostic applications*

Liu Xiao-Li(刘晓丽)[a)b)], Yang Yong(杨 勇)[a)], Wu Jian-Peng(吴建鹏)[b)], Zhang Yi-Fan(张艺凡)[b)], Fan Hai-Ming(樊海明)[b)], and Ding Jun(丁 军)[a)†]

[a)] *Department of Materials Science and Engineering, Faculty of Engineering, National University of Singapore, 7 Engineering Drive 1, Singapore 117574, Singapore*

[b)] *School of Chemical Engineering, Northwest University, Xi'an 710069, China*

(Received 29 July 2015; revised manuscript received 20 August 2015; published online 20 Ocotber 2015)

Recent discoveries in the synthesis and applications of magnetic vortex nanorings/nanodiscs in theranostic applications are reviewed. First, the principles of nanomagnetism and magnetic vortex are introduced. Second, methods for producing magnetic vortex nanorings/nanodiscs are presented. Finally, theranostic applications of magnetic vortex nanorings/nanodiscs are addressed.

**Keywords:** magnetic nanorings/nanodiscs, vortex domain, magnetic resonance imaging, magnetic hyperthermia

**PACS:** 75.75.–c, 75.75.Cd, 87.61.–c, 87.53.Jw **DOI:** 10.1088/1674-1056/24/12/127505

## 1. Introduction

Magnetic nanoparticles have been widely used in a variety of applications, especially in biomedical fields such as magnetic resonance imaging (MRI),[1–5] magnetic separation,[6–10] magnetic hyperthermia therapy,[11–16] and drug delivery.[17–20] With the growing concern for the prevention and treatment of cancer, research into MRI diagnosis and magnetic hyperthermia therapy, which are commonly referred to as "theranostics,"[15] has accelerated. One key issue is to improve the magnetic properties of theranostic agents to achieve early detection and efficient treatment for cancer.[21] Already, superparamagnetic nanoparticles (SPIOs) have been widely investigated as theranostic agents, and some have been commercially available for many years.[22–25] It is widely accepted in this field that a stable suspension for biomedical applications can be achieved only by using SPIOs. The non-superparamagnetic nanoparticles possess remanance which may lead to undesired agglomeration. Unfortunately, small SPIOs with low saturation magnetization have limits in theranostic applications. Designing and optimizing the size, composition, shape, and surface of magnetic nanoparticle coatings is reported to improve the performance of theranostic agents.[4,26–37] However, in the development of these theranostic agents, their efficiency has reached its limit, because their saturation magnetization is comparable to that of bulk materials.[38,39] In addition, introducing other magnetic elements (such as Co and Mn) to increase the magnetic moment may raise concerns about toxicity. Seeking a new class of theranostic agents to replace SPIOs might be an alternative way to solve this problem, but such research encountered a bottleneck in the past. Thus, finding a new approach to design and develop magnetic nanoparticles with good suspension and improved magnetic properties as well as significantly enhanced theranostic performance is becoming important and urgent.

At nanoscale, size and shape effects play important roles in the magnetic properties of nanostructures.[40–42] The size effect results in single-domain ferromagnetic/ferrimagnetic and superparamagnetic nanoparticles, which have attracted intense interest due to their extraordinary potential for biomedical applications. When shape changes at a nanoscale, new magnetization configurations appear. Different shapes prefer different magnetic domain structures for energy minimization, leading to tremendous variation in magnetic properties. To fully exploit the size and shape effects at nanoscale and realize optimum properties for targeted applications, the understanding of nanomagnetism, control of magnetic properties and development of related synthetic methods are of great importance.

The discovery of magnetic vortex-domain nanorings/nanodiscs has brought a novel approach for forming a good suspension and improving magnetic properties. To achieve a stable vortex-domain structure, the dimensions of the nanorings/nanodiscs must be carefully manipulated. For example, outer diameter, height and inner-to-outer diameter ratio are the key parameters for nanorings to be located in the exact region of the stable vortex area.[43] In particular, this unique magnetic structure endows nanorings/nanodiscs with

*Project supported by the National Natural Science Foundation of China (Grant Nos. 21376192 and 81571809), the Research Fund for the Doctoral Program of Higher Education of China (Grant No. 20126101110017), and MOE AcRF Tier 2-MOE2011-T2-1-043 and A-Star SERC 1321202068.

†Corresponding author. E-mail: msedingj@nus.edu.sg

© 2015 Chinese Physical Society and IOP Publishing Ltd 

negligible or decreased remanence and coercivity — greatly reducing dipole–dipole interactions and enabling good colloidal stability — but with much higher saturation magnetization and larger hysteresis loops than SPIOs. Under an external field, nanorings/nanodiscs undergo magnetic moment reversal processes and move along the field direction rapidly. Therefore, nanorings/nanodiscs with magnetic vortex-domain structure have emerged as a new material for theranostic applications.

In this review, we aim to provide an overview of recent developments in the chemical synthesis of magnetic vortex-domain nanorings/nanodiscs and developments in their applications. We first introduce the general principles of nanomagnetism and magnetic vortex-domain. We then discuss chemical synthesis of magnetic vortex-domain nanorings/nanodiscs. Toward the end, the potential applications of the nanorings/nanodiscs in biomedicine are highlighted.

## 2. General principles

Characterization of magnetic nanoparticles might address many magnetic properties. The basic properties are the types of response to a magnetic field (including ferromagnetic/ ferrimagnetic/superparamagnetic, paramagnetic and antiferromagnetic).[44,45] The magnetization curve characterizes this magnetic behavior of magnetic nanoparticles. For ferromagnetic/ferrimagnetic materials, the magnetic properties are typically of interest, such as saturation magnetization ($M_s$), remanence magnetization ($M_r$) and coercivity ($H_c$) can be obtained from the hysteresis loop (Fig. 1(a) and Fig. 1(d)). Figure 1(b) illustrates the dependence of coercivity on particle size. To minimize its magnetostatic energy, a ferromagnetic/ferrimagnetic particle needs to possess multiple magnetic domain structures. For particles smaller than a certain critical value, the energy required to create a domain wall is greater than the demagnetizing energy, enforcing a single-domain state. In this state, coercivity reaches a maximum at critical size, associated with the transition from multi-domain to the single domain. Further decreasing particle size results in a steep decrease of the $H_c$ due to the assistance of thermal energy $k_BT$ ($k_B$ and $T$ are the Boltzmann constant and temperature) in the switching process.[42] When particle size is reduced to a level where the magnetic anisotropy energy ($KV$) ($K$ and $V$ are the effective anisotropy constant and the nanoparticle volume) is much smaller than $k_BT$, the spins rotate freely, without

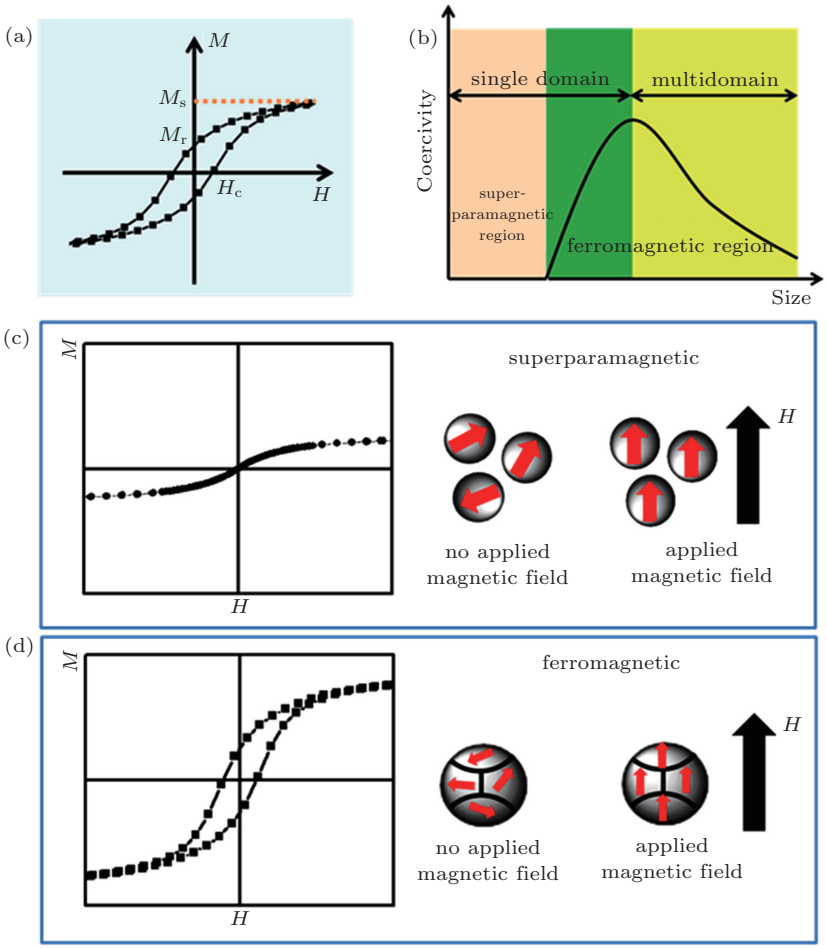



**Fig. 1.** (color online) (a) A typical hysteresis loop of a ferromagnetic/ferrimagnetic material. (b) Schematic illustration of the dependence of coercivity on particle size. (c) and (d) Typical hysteresis loops of a superparamagnetic nanomaterial and a ferromagnetic/ferrimagnetic nanomaterial. Under a magnetic field, the magnetic moments of the domains of ferromagnetic particles and single-domain superparamagnetic particles are aligned. After removal of the magnetic field, ferromagnetic particles maintain a net magnetization.

any external field. Such a nanoparticle is said to be superparamagnetic. As shown in Fig. 1(c), the $M$–$H$ curve of SPIOs shows no hysteresis. The forward and backward magnetization curves coincide completely and the area is almost negligible, indicating the anhysteretic nature. Magnetic nanoparticles in a superparamagnetic state do not tend to agglomerate, enabling suspension of the particles. Most experimental work in this field to date has used SPIOs. However, SPIOs' weak magnetic interaction offsets their $M_s$.[30] Moreover, the usefulness of SPIOs suffers from surface effects, due to their high specific surface, which also offsets $M_s$, because of surface spin disorder in this case.[46] In addition, due to the decreased saturation magnetization, high magnetic fields, which may harm the human body, are required to manipulate these nanoparticles. Conversely, if magnetic particles with high saturation magnetization are fabricated, agglomeration may occur, owing to the large $M_r$. As shown in Figs. 1(c) and 1(d), under an applied magnetic field, the magnetic moment of the domains of ferromagnetic/ferrimagnetic particles and single-domain superparamagnetic particles are aligned. After removal of the applied magnetic field, ferromagnetic/ferrimagnetic particles maintain a net magnetization.

Magnetic vortex structures offer a new opportunity to achieve stable suspension and high saturation magnetization simultaneously. The hysteresis loop of a magnetic vortex nanoring is shown in Fig. 2(d). Due to the enclosed domain without stray fields, the $M_r$ and $H_c$ of magnetic vortex nanorings are close to zero. At the same time, in comparison with SPIOs, the magnetic vortex nanoring, larger in size, has a much higher $M_s$. This makes magnetic vortex nanostructures a promising candidate for diverse biomedical applications.

The flux-closure vortex domain structure, where the spins align circularly, is a common magnetic state in magnetic nanorings/nanodiscs and has been intensively studied.[47–60] In particular, the vortex-domain structure is sensitive to nanoring dimensions.[43] Our group has performed three-dimensional (3D) Landau–Liftshitz–Gilbert (LLG) micromagnetic simulations for magnetite nanorings. Figures 2(a)–2(c) illustrate the observed remanence states of the magnetite nanorings within the vortex region of the ground state phase diagram at $\beta = 0.4$, 0.6 and 0.8 ($\beta = D_{in}/D_{out}$) with the applied magnetic field along the $x$ direction. The symbols represent computed points. We concluded that only the few areas highlighted by dashed lines were stable vortex areas.

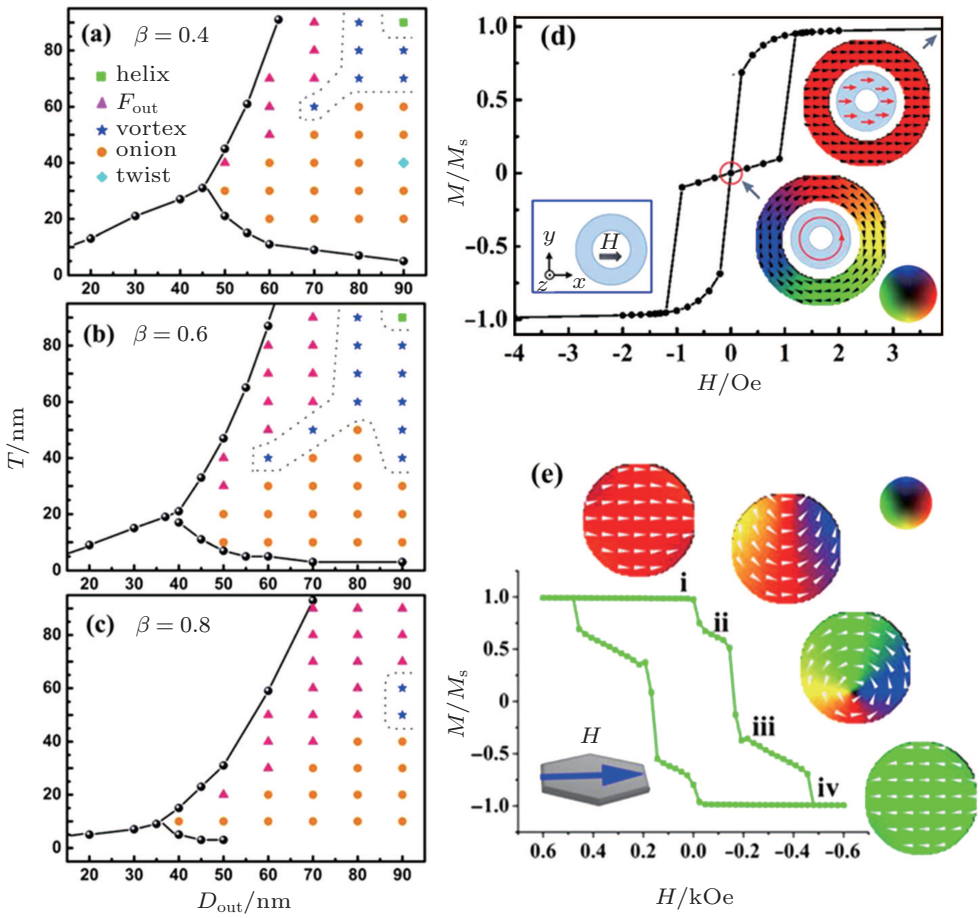



**Fig. 2.** (color online) (a)–(c) Observed remanence states of the magnetite nanorings within the vortex region of the ground state phase diagram at $\beta =$ (a) 0.4, (b) 0.6, (c) 0.8.[43] Reprinted with permission from Ref. [43]; Copyright 2012, AIP Publishing, LLC. (d)–(e) Magnetic states during switching when field is parallel to nanorings[43] and nanodisc[59] The cartoons are schematic diagrams of the corresponding domain structures. The unit 1 Oe = 79.5775 A/m. Reprinted with permission from Ref. [43], copyright 2012, AIP Publishing, LLC. Reprinted with permission from Ref. [59], © 2014 WILEY-VCH Verlag GmbH & Co. KGaA, Weinheim.

Under an external magnetic field, the magnetic vortex state transforms into another state, which is closely related to the geometric shape of the nanomaterials.[47,48] Figures 2(d) and 2(e) provide examples of reversal processes in magnetic nanorings and nanodiscs, simulated by Yang *et al*. For magnetic vortex-domain nanorings, the hysteresis loop is typically of a two-step magnetization reversal process involving an onion-to-vortex transition and then a transition from vortex to the reverse onion state.[43,61,62] As illustrated in Fig. 2(d), at $H = 0$ (vortex state), the magnetization circulates around the ring without stray field. As $H$ increases, a new magnetic domain with opposite chirality nucleates. When $H$ is larger than the switching field $H_s$, the onion state appears with two opposite head-to-head domain walls. Figure 2(e) presents a domain evaluation of a nanodisc. Obviously, at $H = 0$, the transition occurs from saturation state (i) to the c-state (ii). As $H$ increases, a vortex core moves in from the edge of the nanodisc and forms a vortex state (iii). When H further increases, the vortex core moves gradually toward the opposite edge. The nanodisc is saturated until the vortex core disappears (iv). In contrast to magnetic vortex-domain nanodiscs with high energy vortex core, the vortex state in rings is a stable magnetic configuration. Based on the theory simulation of magnetic vortex-domain colloid, Fan *et al.* were first to propose a colloid of magnetic vortex nanorings for biomedical applications.[43,63,64] The $M$–$H$ curve (Fig. 2(d)) reveals there is no remanence for magnetic vortex nanorings. For fields sweeping from positive to negative saturation, the onion state maintains at remanence and the transition from onion to vortex state occurs abruptly at a certain field. The vortex state leads to weak magnetic interactions of nanorings that can be utilized to facilitate a magnetic nanoring suspension. The unique vortex structure and high saturation magnetization can provide strong local field inhomogeneity and large hysteresis, resulting in an extremely large $r_2^*$ relaxivity in MRI and extremely large specific absorption rate (SAR) in magnetic hyperthermia, respectively. In addition, a dispersion consisting of vortex nanorings can provide a fast, strong response under relatively small external field to meet the increasing demands of biological applications.

## 3. Fabrication of magnetic vortex-domain nanorings/nanodiscs

Controllable synthesis of magnetic nanorings/discs is a key for forming a stable vortex-domain structure and pursuing its biomedical applications. The prevailing strategy for preparing magnetic nanorings/discs is the solvothermal method.[54,65–68]

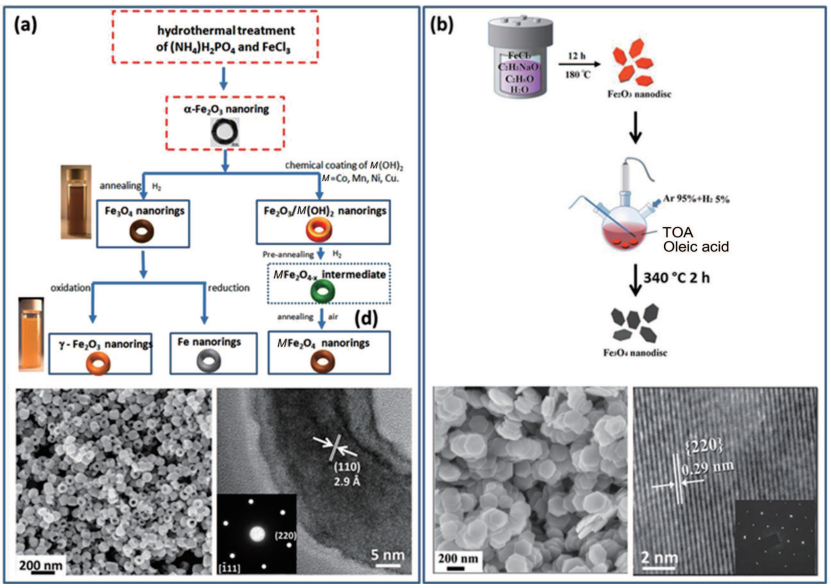



**Fig. 3.** (color online) (a) (top) Typical synthesis of magnetic nanorings; (bottom) SEM image and HRTEM of prepared $Fe_3O_4$ nanorings; inset is a selected area electron diffraction (SAED) image[64] Reprinted with permission from Ref. [64], © 2015 WILEY-VCH Verlag GmbH & Co. KGaA, Weinheim. (b) (top) Schematic illustration for the synthesis of $Fe_3O_4$ nanodiscs;[59] (bottom) SEM image and HRTEM of prepared $Fe_3O_4$ nanodiscs; inset is an SAED image[59] Reprinted with permission from Ref. [59], © 2014 WILEY-VCH Verlag GmbH & Co. KGaA, Weinheim.

Single-crystalline magnetic nanorings were fabricated by hydrothermal growth of hematite ($\alpha$-$Fe_2O_3$) nanorings and post reduction. Fan *et al.*[65,66] reported that $\alpha$-$Fe_2O_3$ nanorings could be formed through hydrothermal treatment of $FeCl_3$ in the presence of $NH_4H_2PO_4$. In this case, $NH_4H_2PO_4$ could covalently adsorb onto $\alpha$-$Fe_2O_3$ crystal planes parallel to the c axis and react with $\alpha$-$Fe_2O_3$ to form a dissolvable complex in solution, which can serve as either a surfactant to induce anisotropic growth or an etching agent. As a result, hollow nanorings can be obtained during this coordination-assisted

dissolution process. By varying the concentration of $FeCl_3$ and $NH_4H_2PO_4$, the size of hematite nanorings can be modulated. Figure 3(a) shows the overall scheme for the synthesis of spinel $MFe_2O_4$ nanorings. The insets are optical images of $Fe_3O_4$ and $\alpha$-$Fe_2O_3$ nanorings. The obtained $\alpha$-$Fe_2O_3$ nanorings can be further transformed into cubic spinel magnetite $Fe_3O_4$, maghemite $\gamma$-$Fe_2O_3$ or ferrite $MFe_2O_4$ ($M$ = Co, Mn, Ni, Cu) by using a thermal transformation process, without changing their size and shape. Both the scanning electron microscope (SEM) and high-resolution transmission electron microscope (HRTEM) analysis reveal that the as-prepared $Fe_3O_4$ nanorings have uniform size and shape and a single crystal nature.

High quality $Fe_3O_4$ nanodiscs are fabricated by a two-step chemical synthesis, as shown in Fig. 3(b). Chen *et al.*[68] were first to report an alcohol-thermal reaction for the fabrication of uniform $\alpha$-$Fe_2O_3$ nanodiscs. Hexagonal $\alpha$-$Fe_2O_3$ nanodiscs have been successfully grown via a simple ethanol-thermal route in the presence of ethanol with the addition of acetate sodium. Acetate anions in acetate sodium can covalently adsorb onto $\alpha$-$Fe_2O_3$ (0001) surfaces and control the growth along the specific direction. The size can be finely tuned by the selective use of alcohol solvent with an increasing presence of carbon atoms in the linear alkyl chain. $\alpha$-$Fe_2O_3$ nanodiscs are successfully converted into $Fe_3O_4$ nanodiscs by a hydrogen-wet reduction method. Using this method, high quality $Fe_3O_4$ nanodiscs are fabricated as shown in Fig. 3(b) (bottom).

## 4. The applications of vortex-domain nanorings/nanodiscs

### 4.1. Ferrimagnetic vortex-domain nanorings as $T_2$-weighted contrast agent for diagnostics

Early and accurate diagnosis of diseases is very important, because it makes the treatments simpler and more effective. Unfortunately, many types of cancers are still very difficult to detect until their late stages.[69–71] MRI is one of the most powerful medical diagnosis tools for visualizing biological tissues, the images of which are produced by the difference of the nuclear magnetic relaxation of water protons in the body. This technique can provide images with excellent anatomical details based on the soft tissue contrast and real-time monitoring manner.[19,72–74] To improve the sensitivity, magnetic nanoparticles are employed as contrast agents to increase the difference between pathogenic targets and normal tissues.[75] In other words, the presence of a contrast agent modifies the relaxation rate of surrounding protons and, therefore, changes the signal contrast. There are two types of contrast agents, positive ($T_1$) contrast agents and negative ($T_2$ and $T_2^*$) contrast agents. $T_1$ contrast agents shorten the spin-lattice relaxation time of protons ($T_1$ relaxation time) in the surroundings and generate a bright image; $T_2$ contrast agents shorten the spin–spin relaxation times ($T_2$ relaxation time) leading to signal reduction, that is, a dark image.[76] The efficiency of the contrast agent is quantified through the relaxation rate $R = 1/T$ ($s^{-1}$) and the normalized relaxivity: $r = R$/concentration ($mM^{-1}\cdot s^{-1}$). The higher the relaxivity, the better the contrast effect.

Due to the magnetic inhomogeneity induced by their strong magnetic moment, magnetic nanoparticles are typically $T_2$ agents.[77] For example, SPIOs such as Ferumoxsil are commercial $T_2$ contrast agents. On the basis of a quantum mechanical outer-sphere theory, the $T_2$ relaxivity of iron oxide nanoparticles can be given by[78,79]

$$\frac{1}{T_2} = \frac{\left(256\pi^2\gamma^2/405\right)V^* M_s^2 a^2}{D\left(1+L/a\right)}, \tag{1}$$

where $\gamma$ is the proton gyromagnetic ratio, $V^*$, $M_s$, and $a$ are the volume fraction, saturation magnetization, and radius of a magnetic nanoparticle core, respectively, $D$ is the diffusivity of water molecules surrounding the magnetic nanoparticles and $L$ is the thickness of an impermeable surface coating. According to this equation, the $T_2$ relaxivity of iron oxide nanoparticles increases with the magnetization and the size of iron oxide cores if the total amount of iron, $V^*$, is constant.

SPIOs with size below 20 nm have low saturation magnetization and susceptibility, which directly results in low performance in applications. Moreover, the relatively small size of SPIOs makes it difficult to retain their stoichiometry, size uniformity and magnetism during the complex protocol for water-soluble nanoparticles, which in turn leads to rather poor performance of the $T_2$ relaxivity effect.[63] In this case, Fan *et al.*[63] reported that ferrimagnetic vortex-domain nanorings (FVIOs) with a superior shape-induced vortex magnetic property (Fig. 4(b)) and tunable size (70 nm–200 nm in outer diameter) are expected to provide significant enhancement of an MR $T_2^*$ signal, which may overcome the drawbacks of conventional SPIO imaging agents. The MRI tests of magnetic vortex nanorings were performed using quantum dot (CdSe/ZnS) capped ferrimagnetic vortex-state iron oxide nanorings (QD-FVIO) (Fig. 4(a)). Figure 4(c) shows a qualitative comparison of $T_2^*$-weighted spin-echo MRI of FVIO and commercial Ferucarbotran regarding the varied echo time. Obviously, compared with Ferucarbotran, QD-FVIOs result in significantly darker images at the designated echo time. The MR relaxivities of QD-FVIOs and Ferucarbotran are presented in Table 1. The $r_2^*$ values and $r_2^*/r_1$ ratios of QD-FVIOs are almost 4-fold and two orders larger than those of the commercial Ferucarbotran, respectively. Previous studies reported that the $r_2^*$ value strongly depends on the inhomogeneity of the local field surrounding the magnetic core, which corresponds to the relative volume fraction, magnetic moment and susceptibility of

magnetic core. Hence, because of its special ring shape and magnetic moment switching process (from vortex to onion), QD-FVIOs possess both high relative volume fraction and susceptibility, which result in the extremely large $r_2^*$ value. In addition, the susceptibility difference between the inner and outer surface of FVIOs could result in the field inhomogeneity, which may also contribute to the enhancement of $r_2^*$ value. Overall, MRI measurements show that FVIO nanoring can significantly enhance $T_2^*$-weighted MRI signals and have potential for cancer imaging applications.

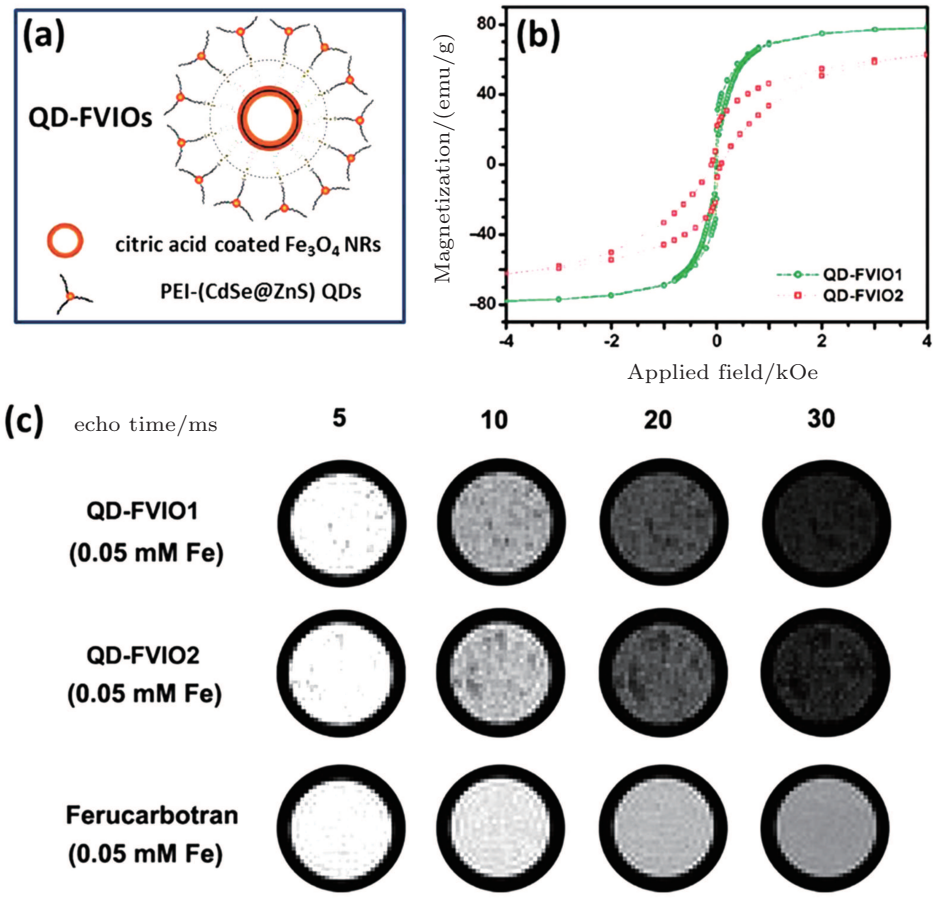



**Fig. 4.** (color online) (a) Schematic illustration of water-dispersible QD-FVIOs. (b) Hysteresis loops of QD-FVIOs at 300 K. (c) *In vitro* $T_2^*$ weighted MRI of QD-FVIOs in 2% agarose and commercial ferucarbotran in water.[63] Reprinted with permission from Ref. [63], Copyright (2010) American Chemical Society.

**Table 1.** MR relaxivities of QD-FVIOs and Commercial Ferucarbotran at 1.5 T[63] Reprinted with permission from Ref. [63]. Copyright (2010) American Chemical Society.

| Sample | $r_1/s^{-1}\cdot mM^{-1}$ | $r_2/s^{-1}\cdot mM^{-1}$ | $r_2/r_1$ | $r_2^*/s^{-1}\cdot mM^{-1}$ | $r_2^*/r_1$ |
|---|---|---|---|---|---|
| QD-FVIO1 | 0.44 | 73.8 | 16 | **1079** | **2450** |
| QD-FVIO2 | 0.59 | 55.1 | 93 | 97 | 1654 |
| Ferucarbotra | 11.3 | 22 | 19.9 | 25 | 22.5 |

### 4.2. Ferrimagnetic vortex-domain nanorings as mediators for anti-tumor therapeutics

Magnetic hyperthermia is a promising therapeutic tool for malignant tumor treatment by converting electromagnetic energy into heat using magnetic nano-mediators.[80,81] This is based on the evidence that cancer cells are more sensitive than normal cells to temperatures higher than 42 °C.[82] Such therapeutic capability is evaluated by SAR. The higher the SAR value, the greater the efficiency. The aim is to enhance the SAR of nano-mediators with a lower dosage. SPIOs are widely used in magnetic hyperthermia investigations because of their superparamagnetism, stable suspension and large surface area.[83,84] However, magnetic nanoparticles possess low saturation magnetization and susceptibility, which in turn has affected its performance in applications. In addition to currently available SPIOs, the difficulty in striking a balance between having a good suspension and improved magnetic properties presents a challenging obstacle for the development of high-performance magnetic nanoparticle-based therapeutic agents.

FVIOs possess a ferromagnetic vortex-domain structure with negligible remanence and coercivity that can greatly reduce dipole–dipole interactions and enable good colloidal stability, but they have much higher saturation magnetization than SPIOs and a larger hysteresis loop.

The first magnetic hyperthermia test of magnetic vortex nanorings was performed using PEG ($M_w = 5000$ Da) capped

FVIO. It demonstrated that an FVIO suspension is very efficient for thermal induction. Figure 5(a) shows a comparison of FVIOs and Resovist at 400 kHz. It is clear that FVIOs have far greater conversion efficiency than Resovist has. The highest SAR of FVIOs is 3050 $W \cdot g^{-1}$ Fe at 400 kHz and 740 Oe, which is one order of magnitude higher than that of Resovist (106 $W \cdot g^{-1}$). The high SAR values clearly indicate the excellent heating capability of FVIOs in comparison with single-domain $Fe_3O_4$ nanoparticles. The significantly superior heat generation ability of FVIO suspensions is likely related to a stable magnetic vortex-domain structure, a vortex-to-onion magnetization reversal process, large hysteresis loss and a relatively large $M_s$. Theoretically, the heat induced by magnetic nano-mediators is proportional to the area of their hysteresis loop. Simulated hysteresis loops from an LLG micromagnetism simulation show strong angle-dependence due to shape anisotropy of FVIOs (Fig. 5(b)). Then an *in vivo* anti-tumor experiment was performed. Figure 5(c) shows schematics of magnetic hyperthermia treatment of a tumor in a tumor-bearing nude mouse xenografted with breast cancer cells (MCF-7). Magnetic nanoparticles were directly injected into the tumor of a mouse and an AC magnetic field (37.5 kHz; 400 Oe) was applied for 10 min. It was found that the tumor was eliminated by day 40 after treatment, by measuring the tumor volume (Fig. 5(d)). For comparison, when commercial SPIOs with the same treatment conditions were used to treat the mice, the tumors were not eliminated in 40 days. FVIO suspensions have demonstrated remarkable anti-tumor efficiency in mice without any associated severe toxic effect. The unique vortex-to-onion magnetization reversal process allows FVIOs to possess negligible remanence and significantly superior hysteresis loss, which not only promotes colloid stability but also maximizes the SAR.

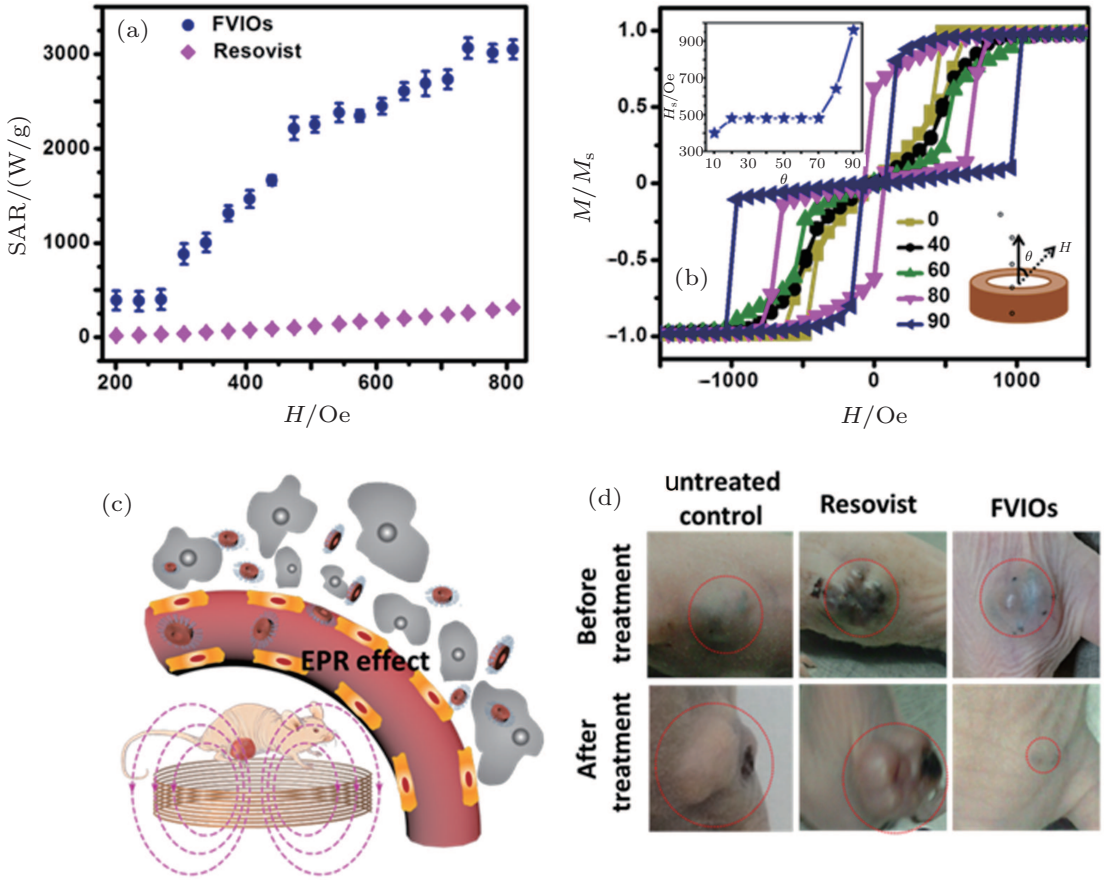



**Fig. 5.** (color online) (a) Comparison of SAR for FVIOs and Resovist in different fields. The frequency is at 400 kHz. (b) Simulated hysteresis loops along different directions. Inset shows the switching field ($H_s$) along different directions. (c) Schematics showing the effect of magnetic hyperthermia treatment on tumor cells in a mouse model. (d) Nude mice xenografted with breast cancer cells (MCF-7) before treatment (upper row, dotted circle) and 40 days after treatment (lower row) with untreated control, Resovist hyperthermia and FVIOs hyperthermia, respectively.[64] Reprinted with permission from Ref. [64], © 2015 WILEY-VCH Verlag GmbH & Co. KGaA, Weinheim.

### 4.3. Ferrimagnetic vortex nanodiscs as mediators for magnetic hyperthermia therapeutics

In addition to the FVIOs, the $Fe_3O_4$ nanodiscs with vortex domain structure were also successfully fabricated and their hyperthermia properties were investigated. As shown in Fig. 6(a), ring-like magnetic flux can be observed in the nanodisc, which implies the existence of a vortex domain structure. From the simulated spin configuration nanodisc, it could

be seen that the majority of spins align circularly in the plane of the disc and the center spin points out of plane, forming a typical vortex domain structure. Based on the domain structures, the hysteresis loops are simulated. Figure 6(b) provides the simulated hysteresis loop. The result is similar with nanorings. It is clear that the hysteresis loop changes significantly at different orientations, implying nanodiscs also have shape-anisotropy. Before measuring magnetic hyperthermia of $Fe_3O_4$ nanodiscs, the heat dissipation due to the hysteresis loss can be computed by[35,85]

$$P = u_0 f \oint M \mathrm{d}H, \tag{2}$$

where $\mu$ is vacuum permeability, $f$ is the frequency (488 kHz) of the alternating current (AC) field and $M$ is the magnetization.

Through the above method, the SARs of nanodiscs in aqueous suspension and in agarose gel (5%) are 4659 W/g and 3017 W/g, respectively. The SAR values match very well with the experimental value of about 4925 W/g in water and 2818 W/g in gel. The excellent agreement between the experimental and calculated SAR values indicates that the SAR value of a nanodisc is strongly related to its orientation. As illustrated in Fig. 6(d), parallel alignment of nanodiscs results in a much higher SAR value than random orientation. In an AC field, nanodiscs in aqueous suspension flip and stir the water, thus converting the field energy into kinetic energy of the surrounding carrier. This study may open a new window for "flipping" based heating seeds for high efficiency magnetic hyperthermia.

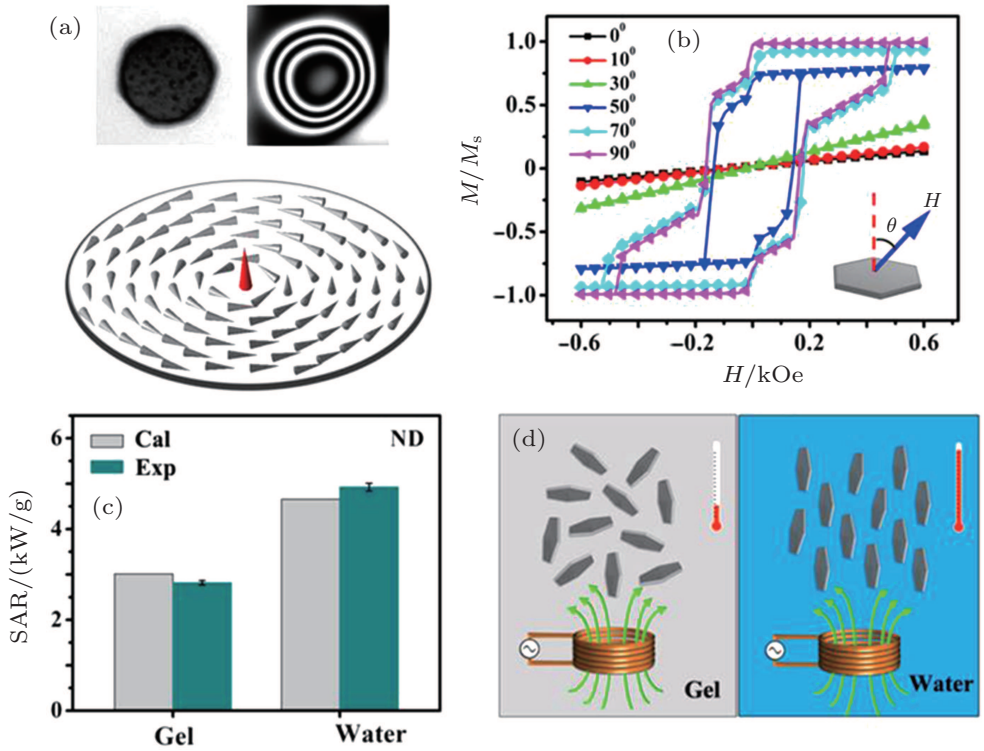



**Fig. 6.** (color online) (a) Magnetic domain structure of nanodisc. (b) Simulated hysteresis loops along different directions. (c) Comparison of SAR values between simulation and experiment in gel and water suspension. (d) Illustration of different orientations of nanodiscs in the gel and water suspension during magnetic hyperthermia measurement.[59] Reprinted with permission from Ref. [59]; © 2014 WILEY-VCH Verlag GmbH & Co. KGaA, Weinheim.

Kim *et al.*[4] also reported novel cancer-treatment strategies using the magnetic vortex properties of magnetic vortex nanodiscs. As reported, the MD-mAb particles, created by combining gold-permalloy (Ni80Fe20) microdiscs and anti-human-IL13$\alpha$2R antibody (mAb), were used to mark N10 glioma cells, which in turn formed MDs-mAb-cell complexes. In an external low frequency AC field, nanodiscs with an unstable vortex core move reciprocally, creating an oscillation which transmits a mechanical force to the cell. Such a mechanical process will repeatedly apply pressure to the membrane of each N10 glioma cell until it shrinks and cracks, ultimately inducing programmed cell death of cancer cells (Fig. 7). To eliminate the influence of thermal effects, an extremely weak AC field (amplitude lower than 100 Oe, frequencies below 60 Hz) is applied, while cell solution temperature is always kept below 22 °C. After applying the field to the N10 glioma for 10 minutes, cancer cells were significantly destroyed, while the surrounding normal tissue was only mildly damaged, as the applied AC field is weak and the application time is short. This research provides a new way of thinking in the treatment of cancer.

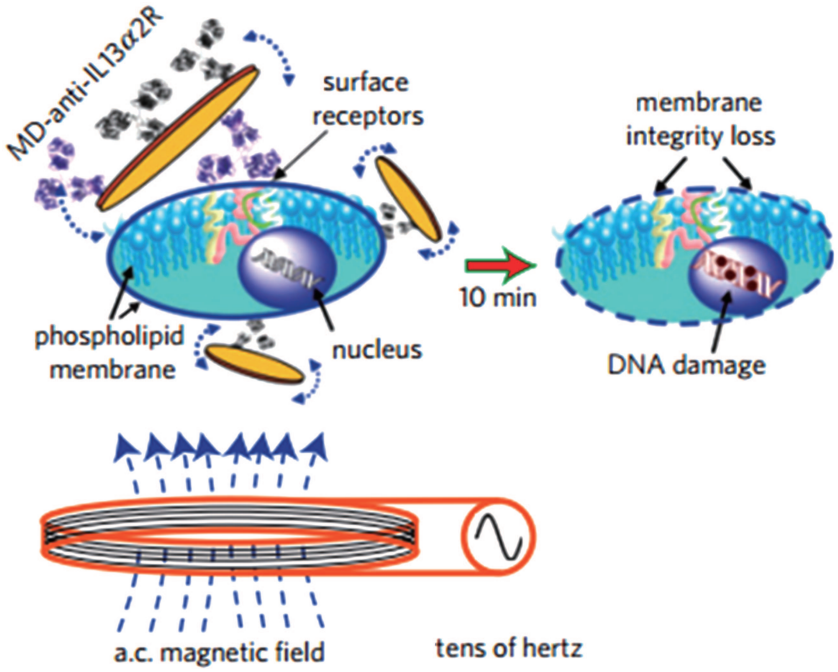



**Fig. 7.** (color online) The concept of targeted magneto mechanical cancer-cell destruction using disc-shaped magnetic particles possessing a spin-vortex ground state.[52] Reprinted with permission from Ref. [52], copyright © 2009; rights managed by Nature Publishing Group.

## 5. Summary and perspective

Exceptional progress has been achieved in synthesis, vortex-domain structure control, and biomedical applications of magnetic vortex nanorings/nanodiscs, as described in this review. Magnetic vortex nanorings/nanodiscs are new platforms for theranostic applications. Chemical synthesis of magnetic nanorings/nanodiscs with vortex domain structure has progressed enormously. Both *in vitro* and *in vivo* studies have demonstrated their potential as diagnostic and therapeutic agents. However, several problems still require considerable work to be solved before magnetic vortex nanorings/nanodiscs are fully established for clinical translation. For example, synthesis of magnetic vortex nanorings/nanodiscs with very small size (10 nm–50 nm) is still challenging. Producing different shapes of nanostructures with vortex-domain magnetic structure is a big problem that needs to be solved. Magnetic vortex domain nanostructure is expected to be functionalized with targeting ligands so that the cellular uptake is more targetable and controllable. The biodistribution, targeting efficiency, toxicity, biodegradability and clearance of magnetic vortex domain nanostructures also need to be studied further. In depth understanding of the magnetic vortex domain will provide a guideline to produce magnetic vortex nanostructures for other applications, such as thermosensitive drug release for cancer treatment. It is expected that magnetic vortex domain structure will be widely applied in magnetic, biomedical and nanotechnology fields.

## References

[1] Hu F Q, Wei L, Zhou Z, Ran Y L, Li Z and Gao M Y 2006 *Adv. Mater.* **18** 2553
[2] Yu J, Yang C, Li J, Ding Y, Zhang L, Yousaf M Z, Lin J, Pang R, Wei L, Xu L, Sheng F, Li C, Li G, Zhao L and Hou Y 2014 *Adv. Mater.* **26** 4114
[3] Liu D, Wu W, Ling J, Wen S, Gu N and Zhang X 2011 *Adv. Funct. Mater.* **21** 1498
[4] Lee J H, Huh Y M, Jun Y W, Seo J W, Jang J T, Song H T, Kim S, Cho E J, Yoon H G, Suh J S and Cheon J 2007 *Nat. Med.* **13** 95
[5] Yang H, Zhang C, Shi X, Hu H, Du X, Fang Y, Ma Y, Wu H, Yang S 2010 *Biomaterials* **31** 3667
[6] Carinelli S, Martí M, Alegret S and Pividori M I 2015 *New Biotechnol.*
[7] Haun J B, Castro C M, Wang R, Peterson V M, Marinelli B S, Lee H and Weissleder R 2011 *Sci. Transl. Med.* **3** 71ra16
[8] Yavuz C T, Mayo J T, William W Y, Prakash A, Falkner J C, Yean S, Cong L, Shipley H J, Kan A, Tomson M, Natelson D and Colvin V L 2006 *Science* **314** 964
[9] Gu H, Xu K, Xu C and Xu B 2006 *Chem. Commun.* **9** 941
[10] Bao J, Chen W, Liu T, Zhu Y, Jin P, Wang L, Liu J, Wei Y and Li Y 2007 *ACS Nano* **1** 293
[11] Hergt R, Dutz S, Müller R and Zeisberger M 2006 *J. Phys.: Condens. Matter* **18** S2919
[12] Kumar C S and Mohammad F 2011 *Adv. Drug. Deliver. Rev.* **63** 789
[13] Laurent S, Dutz S, Häfeli U O and Mahmoudi M 2011 *Adv. Colloid Interface* **166** 8
[14] Yoo D, Lee J H, Shin T H and Cheon J 2011 *Accounts Chem. Res.* **44** 863
[15] Ho D, Sun X and Sun S 2011 *Accounts Chem. Res.* **44** 875
[16] Hao R, Xing R, Xu Z, Hou Y, Gao S and Sun S 2010 *Adv. Mater.* **22** 2729
[17] Arruebo M, Fernández-Pacheco R, Ibarra M R and Santamaría J 2007 *Nano Today* **2** 22
[18] Dobson J 2006 *Drug. Dev. Res.* **67** 55
[19] Sun C, Lee J S and Zhang M 2008 *Adv. Drug. Deliv. Rev.* **60** 1252
[20] Son S J, Reichel J, He B, Schuchman M and Lee S B 2005 *J. Am. Chem. Soc.* **127** 7316
[21] Liu X L and Fan H M 2014 *Curr. Opin. Chem. Eng.* **4** 38
[22] Frimpong R A and Hilt J Z 2010 *Nanomedicine* **5** 1401

[23] Xie J, Huang J, Li X, Sun S and Chen X 2009 *Curr. Med. Chem.* **16** 1278

[24] Guo S, Li D, Zhang L, Li J and Wang E 2009 *Biomaterials* **30** 1881

[25] Kim D K, Mikhaylova M, Wang F H, Kehr J, Bjelke B, Zhang Y, Tsakalakos T and Muhammed M 2003 *Chem. Mater.* **15** 4343

[26] Fortin J P, Wilhelm C, Servais J, Ménager C, Bacri J C and Gazeau F 2007 *J. Am. Chem. Soc.* **129** 2628

[27] Lee N, Choi Y, Lee Y, Park M, Moon WK, Choi SH and Hyeon T 2012 *Nano Lett.* **12** 3127

[28] Guardia P, Di Corato R, Lartigue L, Wilhelm C, Espinosa A, Garcia-Hernandez M and Pellegrino T 2012 *ACS Nano* **6** 3080

[29] Jang J T, Nah H, Lee J H, Moon S H, Kim M G and Cheon J 2009 *Angew. Chem. Int. Ed.* **121** 1260

[30] Lee J H, Jang J T, Choi J S, Moon S H, Noh S H, Kim J W and Cheon J 2011 *Nat. Nanotechnol.* **6** 418

[31] Duan H, Kuang M, Wang X, Wang YA, Mao H and Nie S 2008 *J. Phys. Chem. C* **112** 8127

[32] Tong S, Tong S, Hou S, Zheng Z, Zhou J and Bao G 2010 *Nano Lett.* **10** 4607

[33] Liu X L, Fan H M, Yi J B, Yang Y, Choo E S G, Xue J M and Ding J 2012 *J. Mater. Chem.* **22** 8235

[34] Tromsdorf U I, Bigall N C, Kaul M G, Bruns O T, Nikolic M S, Mollwitz B and Weller H 2007 *Nano Lett.* **7** 2422

[35] Noh S H, Na W, Jang J T, Lee J H, Lee E J, Moon S H and Cheon J 2012 *Nano Lett.* **12** 3716

[36] Liu X L, Choo S G E, Ahmed A S, Zhao L Y, Yang Y, Ramanujan R V, Xue J M, Fan D D, Fan H M and Ding J 2014 *J. Mater. Chem. B* **2** 120

[37] Liu X L, Wang Y T, Ng C T, Wang R, Jing G Y, Yi J B, Yang J, Bay B H, Yung L Y, Fan D D, Ding J and Fan H M 2014 *Adv. Mater. Inter.* **1300069** 1

[38] Vergés M A, Costo R, Roca A G, Marco J F, Goya G F, Serna C J and Morales M P 2008 *J Phys. D: Appl. Phys.* **41** 134003

[39] Lu H M, Zheng W T and Jiang Q 2007 *J Phys. D: Appl. Phys.* **40** 320

[40] Lau J W and Shaw J M 2011 *J. Phys D: Appl. Phys.* **44** 303001

[41] Margeat O, Dumestre F, Amiens C, Chaudret B, Lecante P, Respaud M 2005 *Prog. Solid Stat. Chem.* **33** 71

[42] Lacroix L M, Ho D and Sun S 2010 *Curr. Top. Med. Chem.* **10** 1184

[43] Yang Y, Liu X L, Yi J B, Yang Y, Fan H M and Ding J 2012 *J. Appl. Phys.* **111** 044303

[44] Cullity B D and Graham C D 2011 *Introduction to Magnetic Materials* (Wiley IEEE Press) ISBN: 978-1-118-21149-6

[45] Jun Y W, Choi J S and Cheon J 2007 *Chem. Commun.* **12** 1203

[46] Martnez B, Obradors X, Balcells L, Rouanet A and Monty C 1998 *Phys. Rev. Lett.* **80** 181

[47] Cowburn R P, Koltsov D K, Adeyeye A O, Welland M E and Tricker D M 1999 *Phys. Rev. Lett.* **83** 1042

[48] Li S P, Peyrade D, Natali M, Lebib A, Chen Y, Ebels U, Buda L D and Ounadjela K 2001 *Phys. Rev. Lett.* **86** 1102

[49] Shinjo T, Okuno T, Hassdorf R, Shigeto K and Ono T 2000 *Science* **289** 930

[50] Podbielski J, Giesen F, Grundler D 2006 *Phys. Rev. Lett.* **96** 167207

[51] Wachowiak A, Wiebe J, Bode M, Pietzsch O, Morgenstern M and Wiesendanger R 2002 *Science* **298** 577

[52] Kim D H, Rozhkova E A, Ulasov L V, Bader S D, Rajh T, Lesniak M S and Novosad V 2009 *Nat. Mater.* **9** 165

[53] He K, Smith D J and McCartney M R 2010 *J. Appl. Phys.* **107** 09D307

[54] Jia C J, Sun L D, Luo F, Han X D, Heyderman L J, Yan Z G, Yan C H, Zheng K, Zhang Z, Takano M, Hayashi N, Eltschka M, Kläui M, Rüdiger U, Kasama T, Gontard L C, Dunin-Borkowski R E, Tzvetkov G and Raabe J 2008 *J. Am. Chem. Soc.* **130** 16968

[55] Neudecker I, Kläui M, Perzlmaier K, Backes D, Heyderman L J, Vaz C A F, Bland J A C, Rüdiger U and Back C H 2006 *Phys. Rev. Lett.* **96** 057207

[56] Kläui M, Jubert P O, Allenspach R, Bischof A, Bland J A C, Faini G, Rüdiger U, Vaz C A F, Vila L and Vouille C 2005 *Phys. Rev. Lett.* **95** 026601

[57] Rothman J, Kläui M, Lopez-Diaz L, Vaz C A F, Bleloch A, Bland J A C, Cui Z and Speaks R 2001 *Phys. Rev. Lett.* **86** 1098

[58] Lua S Y H, Kushvaha S S, Wu Y H, Teo K L and Chong T C 2008 *Appl. Phys. Lett.* **93** 122504

[59] Yang Y, Liu X, Lv Y, Herng T S, Xu X, Xia W, Zhang T, Fang J, Xiao W and Ding J 2015 *Adv. Funct. Mater.* **25** 812

[60] Tanigaki T, Takahashi Y, Shimakura T, Akashi T, Tsuneta R, Sugawara A and Shindo D 2015 *Nano Lett.* **15** 1309

[61] Lopez-Diaz L, Kläui M, Rothman J and Bland J A C 2002 *J. Magn. Magn. Mater.* **242** 553

[62] Kazakova O, Hanson M, Blixt A M and Hjörvarsson B 2003 *J. Magn. Magn. Mater.* **258** 348

[63] Fan H M, Olivo M, Shuter B, Yi J B, Bhuvaneswari R, Tan H R, Xing G C, Ng C T, Liu L, Lucky S S, Bay B H and Ding J 2010 *J. Am. Chem. Soc.* **132** 14803

[64] Liu X L, Yang Y, Ng C T, Zhao L Y, Zhang Y, Bay B H, Fan H M and Ding J 2015 *Adv. Mater.* **27** 1939

[65] Fan H M, You G J, Li Y, Zheng Z, Tan H R, Shen Z X, Tang S H and Feng Y P 2009 *J. Phys. Chem. C* **113** 9928

[66] Fan H M Yi J B, Yang Y, Kho K W, Tan H R, Shen Z X, Ding J, Sun X W, Olivo M C and Feng Y P 2009 *ACS Nano* **3** 2798

[67] Lu J, Jiao X, Chen D and Li W 2009 *J. Phys. Chem. C* **113** 4012

[68] Chen L Q, Yang X F, Chen J, Liu J, Wu H, Zhan H, Liang C and Wu M 2010 *Inorg. Chem.* **49** 8411

[69] Cancer: Key Facts. Retrieved 18th December 2013, from http://www.who.int/mediacentre/factsheets/fs297/en/

[70] Sailor M J and Park J H 2012 *Adv. Mater.* **24** 3779

[71] Nguyen K T 2011 *J. Nanomed. Nanotechnol.* **2** 5

[72] Deng C L, Poggio M, Mamin H J, Rettner C T and Rugar D 2009 *Proc. Natl. Acad. Sci. USA* **106** 1313

[73] Weissleder R and Pittet M J 2008 *Nature* **452** 580

[74] Jun Y W, Lee J H and Cheon J 2008 *Angew. Chem. Int. Ed.* **47** 5122

[75] Qiao R R, Yang C H and Gao M Y 2009 *J. Mater. Chem.* **19** 6274

[76] Kim B H, Lee N, Kim H, An K, Park Y I, Choi Y, Shin K, Lee Y, Kwon S G, Na H B, Park J G, Ahn T Y, Kim Y W, Moon W K, Choi S H and Hyeon T 2011 *J. Am. Chem. Soc.* **133** 12624

[77] Huh Y M, Jun Y, Song H T, Kim S, Choi J, Lee J H, Yoon S, Kim K S, Shin J S, Suh J S and Cheon J 2005 *J. Am. Chem. Soc.* **127** 12387

[78] Gillis P, Moiny F and Brooks R A 2002 *Magn. Reson. Med.* **47** 257

[79] Brooks R A, Moiny F and Gillis P 2001 *Magn. Reson. Med.* **45** 1014

[80] Jordan A, Wust P, Fahling H, John W, Hinz A and Felix R 1993 *Int. J. Hyperthermia* **9** 51

[81] Rosensweig R E 2002 *J. Magn. Magn. Mater.* **252** 370

[82] Hamdan S 2013 *International Journal of Chemical, Environmental & Biological Sciences* **1** 191

[83] Gupta A K and Gupta M 2005 *Biomaterials* **26** 3995

[84] Paul A 2004 *Nat. Biotechnol.* **22** 47

[85] Carrey J, Mehdaoui B and Respaud M 2011 *J. Appl. Phys.* **109** 083921